A R C H I V E S O F M E T A L L U R G Y A N D M A T E R I A L S
Volume 58 2013 Issue 2
DOI: 10.2478/v10172-012-0195-0

K. STAN*, L. LITYŃSKA-DOBRZYŃSKA*, P. OCHIN**, A. WIERZBICKA-MIERNIK*, A. GÓRAL*, J. WOJEWODA-BUDKA*

EFFECT OF ALLOYING ELEMENTS ON MICROSTRUCTURE AND PROPERTIES OF Al-Mn-Fe RIBBON

WPŁYW DODATKÓW STOPOWYCH NA MIKROSTRUKTURĘ I WŁASNOŚCI SZYBKO CHŁODZONYCH TAŚM STOPU Al-Mn-Fe

Influence of Ti, V, Cr, Zr, and Mo additions on microstructure and mechanical properties of the $Al_{91}Mn_7Fe_2$ quasicrystalline alloy produced by the melt spinning technique has been studied. It was found that the microstructure of obtained all ribbons was similar and consists of spherical or dendritic icosahedral quasicrystalline particles embedded in an aluminium matrix coexisting with small fraction of intermetallic phase. Comporing DSC curves obtained for each sample it was observed that the alloy with Mo addition exhibits the best thermal stability among prepared alloys. Addition of molybdenum caused a significant shift of the main exothermic peak corresponding to temperature of quasicrystalline phase decomposition from 450°C for ternary alloy to about 550°C for quaternary composition. Microhardness measured for all prepared alloys were similar with the mean value of about 200 HV only alloy with Zr addition exhibited higher microhardness of about 270 HV caused by strengthening effect of Zr localized in the grains of aluminium matrix.

Keywords: quasicrystals, aluminium alloys, Al-Mn-Fe, rapid quenching, TEM, DSC

W niniejszej pracy badano wpływ dodatków stopowych: Ti, V, Cr, Zr i Mo na mikrostrukturę oraz własności mechaniczne kwazikrystalicznego stopu $Al_{91}Mn_7Fe_2$ przygotowanego metodą odlewania na wirujący walec (melt spinning). Uzyskane wyniki pokazały, że mikrostruktura wszystkich otrzymanych taśm była zbliżona i zawierała sferyczne lub dendrytyczne cząstki kwazikrystaliczne umieszczone w osnowie aluminiowej wraz z niewielką ilością fazy międzymetalicznej. Porównując krzywe DSC dla każdej z próbek zaobserwowano, że stop z dodatkiem molibdenu wykazuje najlepszą stabilność termiczną pośród odlanych stopów. Dodatek tego pierwiastka spowodował znaczące przesunięcie głównego piku egzotermicznego związanego z rozpadem fazy kwazikrystalicznej o około 100°C, to jest od temperatury 450°C dla stopu trójskładnikowego do temperatury 550°C dla stopu czteroskładnikowego. Wartości mikrotwardości zmierzone dla każdego ze stopów były zbliżone a ich średnia wartość wynosiła 200 HV. Wyjątek stanowił stop z dodatkiem Zr dla którego średnia wartość mikrotwardości wynosiła 270 HV ze względu na efekt umacniający, związany z obecnością cyrkonu w ziarnach osnowy.

1. Introduction

Recently, a group of high strength and thermally stable aluminium base alloys with microstructure containing finely dispersed nano-size quasicrystalline particles embedded in an aluminium solid solution matrix has been strongly investigated [1-3]. Some of the first results concerning these alloys reported the value of tensile fracture strength exceeding 1000 MPa for Al-Mn-Ce alloy [4]. Alloys with mentioned structure can be obtained for composition with more than 90 at.% of Al and with addition of two or more transition elements. Production of such materials involves rapid quenching methods which enable formation of the metastable quasicrystalline phase in Al-TM systems. Addition of transition metals as alloying elements also provides good thermal stability of the alloy considered as maintaining its specific microstructure, and therefore the mechanical properties even after prolonged heating at elevated temperatures [5]. This effect is connected with low diffusivity of the transition elements in Al which is responsible for retarded decomposition of the strengthening phase during heating - in this case quasicrystalline phase. Combination of high strength and ability to work at higher temperature range without deterioration of alloy mechanical properties is of great interest in terms of potential industrial applications. At present 7xxx series alloys with the best mechanical properties (tensile strength of about 700 MPa) usually to operate at room temperatures. For these alloys deterioration of mechanical properties occurs at about 150°C [6]. Even for Al-Si base alloys commonly used at higher temperature, the value of UTS at 300°C is about 200-250 MPa [7-9], while for nanoquasicrystalline aluminium alloys reported value at 350°C was 440 MPa for Al-Fe-Cr-Ti alloy [1]. The temperature of quasicrystalline phase decomposition should be above 400°C when considering a route of formation of bulk materials by compaction of atomized powders or pulverized ribbons e.g. by extrusion or hot pressing is considered. With a proper combination of alloying elements, the stability of quasicrystalline phase in the alloy can be maintained up to 550°C for

* INSTITUTE OF METALLURGY AND MATERIALS SCIENCE POLISH ACADEMY OF SCIENCES, 30-059 KRAKOW, 25 REYMONTA ST., POLAND
** INSTITUT DE CHIMIE ET DES MATÉRIAUX PARIS EST, CNRS-UNIVERSITÉ PARIS XII, 2-8 RUE HENRI DUNANT, 94320 THIAIS, FRANCE

some compositions [10]. In the literature, quasicrystalline alloys based on Al-Cr [2-3, 11] and Al-Fe [12-17] systems are most extensively investigated, in particular the effect of subsequent alloying elements on their microstructure and properties. The most common additions are V, Ti, and Si [1-3]. Some of these alloys have been also produced in a bulk form [2, 3, 5].

For the Al-Mn system, influence of alloying elements such as Be [18], Sr [19] and Ce [20] has been studied. It has been also reported that Al-Mn base alloy with iron addition exhibits promising mechanical properties with the tensile fracture strength of 1250 MPa [21]. However, the stability of quasicrystalline phase in this alloy was the lowest among the systems (Al-Cr and Al-V) studied in mentioned work. Since there is a lack of information about improvement of alloy properties including its thermal stability, more detailed research are carried out. This work is a continuation of the studies on the quasicrystalline alloys based on Al-Mn-Fe system [22-23]. In this paper an influence of addition of fourth alloying element on the microstructure and mechanical properties of the $Al_{91}Mn_7Fe_2$ alloy, as well as its thermal stability are investigated. With the aim of producing desired microstructure, transition metals were chosen as the subsequent alloying elements according to previous considerations of their ability to form quasicrystalline phase, as well as concerning their low diffusion coefficient in aluminium which influences alloy thermal stability.

2. Experimental procedure

The alloys of nominal compositions $Al_{91}Mn_6Fe_2X_1$ (X= Zr, Cr, Ti, V and Mo) were prepared using high-purity elements: 99.99% Al, 99.99% Fe, 99.99% Mn (purity of fourth alloying element, marked as X, was at least 99.95%). The ternary $Al_{91}Mn_7Fe_2$ alloy was taken as a reference material. All alloys were induction melted in vacuum and then cast into steel mould. The nominal chemical composition of the prepared alloys, together with composition measured by EDX in SEM, as well as the alloy designations are presented in Table 1. The ingots were re-melted and rapidly solidified using the melt-spinning technique. The melt was ejected from a quartz crucible with a nozzle in the bottom onto a copper wheel rotating at linear velocity v = 20 m/s under helium atmosphere. The pressure of the gas ejecting the molten alloy was 180 mbar. The ribbons cast under these conditions were 20-40 μm thick and about 10 mm broad.

Phase characterization of the melt spun ribbons was performed by X-ray diffraction (XRD) using Philips PW 1840 X-ray diffractometer with CoK_α radiation. Microstructure observation and chemical composition analysis were carried out using scanning electron microscopy (SEM, FEI E-SEM XL30) equipped with an energy dispersive X-ray spectrometer (EDX) and transmission electron microscopy (TEM, FEI Tecnai G^2) operating at 200 keV and combined with high-angle annular dark field scanning transmission electron microscopy detector (HAADF-STEM) as well as energy dispersive X-ray spectrometer (EDAX). The Tenupol-5 double jet electropolisher was used for the preparation of thin foils in electrolyte containing nitric acid and methanol (1:3), at the temperature of -30°C and voltage of 15 V. Thermal stability of melt spun ribbons was analyzed by differential scanning calorimetry (DSC, Du Pont 910) with the heating rate of 40 K/min in the argon protective atmosphere. Microhardness was measured with the CSM Microhardness Tester with load 0.1 N (contact load – 0.01 N).

3. Results and discussion

The microstructure of all investigated ribbons was studied by SEM observation of their longitudinal cross section (Fig. 1). Thickness of the ribbons measured on SEM images varies in the range 20-40 μm and changes over the ribbons length. In most cases the formation of two typical areas within the ribbon was noticed. Wheel side usually contained fine spherical particles (less than 1 μm), while dendrites with significantly larger size (from one to several μm) were formed at the air side. It is generally assumed that formation of these two zones is the result of different cooling rates within the both sides of ribbon (air and wheel side) during solidification.

TABLE 1

Alloys designation and nominal chemical compositions of the prepared ingots together with an average values of the elements content measured by EDX in SEM; (X = Zr, Cr, Ti, V or Mo)

Alloy designation	Nominal chemical composition [at.%]	Chemical composition measured by EDX [at. %]			
		Al	Mn	Fe	X
AlMnFe	$Al_{91}Mn_7Fe_2$	90.7±1.8	7.0±0.3	2.3±0.5	-
AlMnFeZr or (Zr)	$Al_{91}Mn_6Fe_2Zr_1$	92.2±1.8	5.0±0.5	1.7±0.4	1.1±0.2
AlMnFeCr or (Cr)	$Al_{91}Mn_6Fe_2Cr_1$	92.2±1.8	5.2±0.5	1.7±0.4	0.9±0.4
AlMnFeTi or (Ti)	$Al_{91}Mn_6Fe_2Ti_1$	91.2±1.8	5.8±0.2	2.0±0.4	1.0±0.2
AlMnFeV or (V)	$Al_{91}Mn_6Fe_2V_1$	92.6±1.9	4.9±0.5	1.7±0.3	0.8±0.4
AlMnFeMo or (Mo)	$Al_{91}Mn_6Fe_2Mo_1$	90.7±1.8	6.1±0.2	2.0±0.4	1.2±0.2

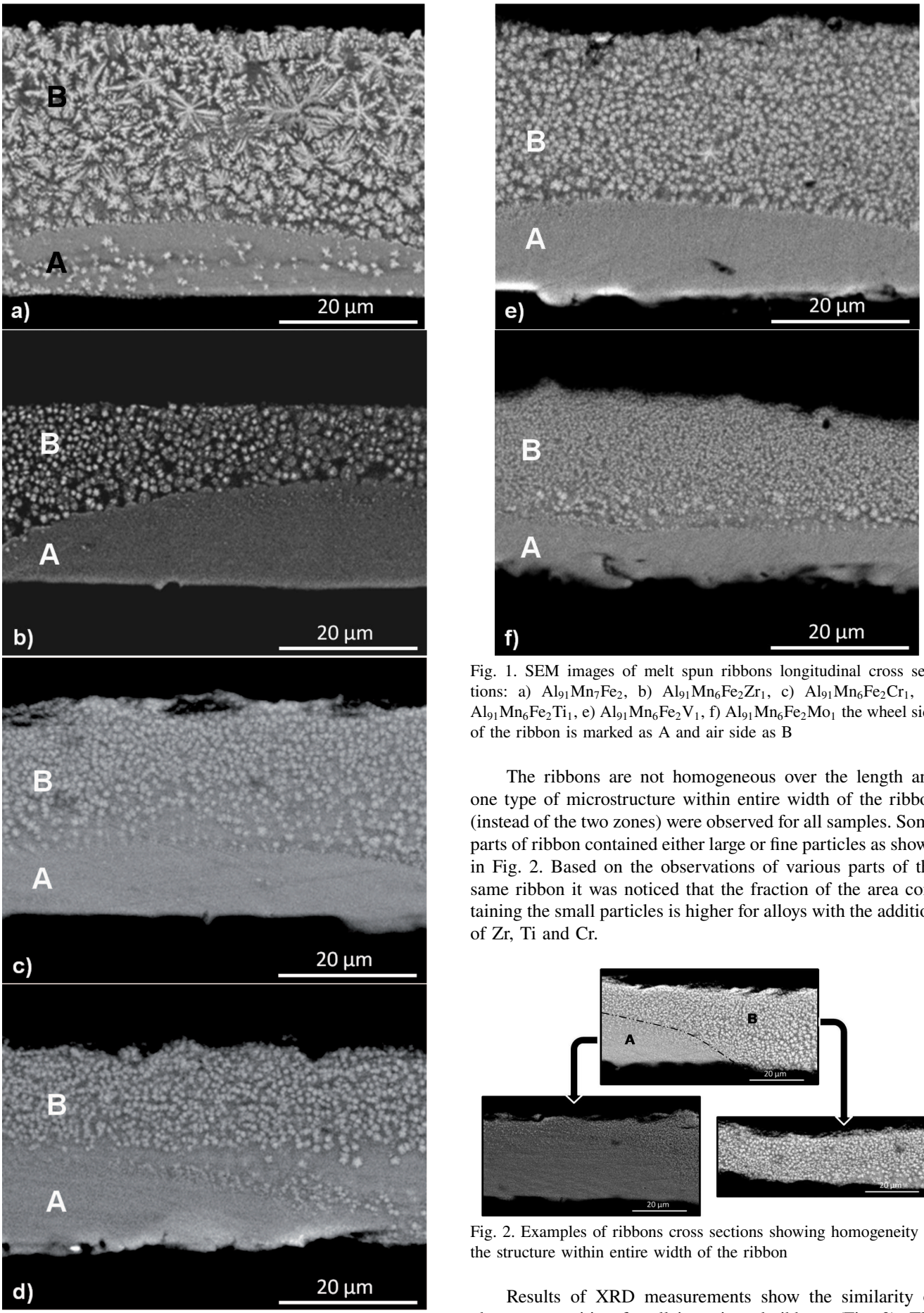

Fig. 1. SEM images of melt spun ribbons longitudinal cross sections: a) $Al_{91}Mn_7Fe_2$, b) $Al_{91}Mn_6Fe_2Zr_1$, c) $Al_{91}Mn_6Fe_2Cr_1$, d) $Al_{91}Mn_6Fe_2Ti_1$, e) $Al_{91}Mn_6Fe_2V_1$, f) $Al_{91}Mn_6Fe_2Mo_1$ the wheel side of the ribbon is marked as A and air side as B

The ribbons are not homogeneous over the length and one type of microstructure within entire width of the ribbon (instead of the two zones) were observed for all samples. Some parts of ribbon contained either large or fine particles as shown in Fig. 2. Based on the observations of various parts of the same ribbon it was noticed that the fraction of the area containing the small particles is higher for alloys with the addition of Zr, Ti and Cr.

Fig. 2. Examples of ribbons cross sections showing homogeneity of the structure within entire width of the ribbon

Results of XRD measurements show the similarity of phase composition for all investigated ribbons (Fig. 3). The strongest reflections which are observed in diffractograms cor-

respond to α(Al) solid solution and quasicrystalline phase. The shift of the position of the quasicrystalline reflections are visible in the enlargement part of the diffractograms (the high shift observed for the samples with V, Ti and Mo addition confirms dissolution of these elements in quasicrystalline phase). For the ribbon containing Zr, the peaks do not shift even though this element has the highest values of atomic radii comparing with other element used (see Table 2, where diffusivity and solid solubility of transition metals in Al, together with their melting points and atomic radius are presented). This indicate that Zr atoms are not involved in the formation of quasicrystalline phase in this system and remain in the matrix.

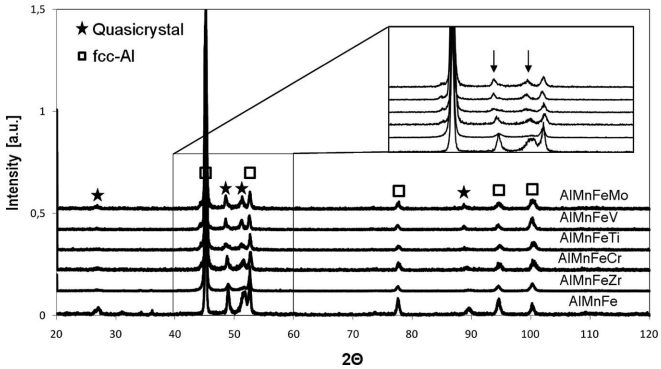

Fig. 3. Diffractograms revealing similarity in phase composition for all investigated ribbons

TABLE 2
Diffusivity and solid solubility of transition metals in Al, together with their melting points and atomic radius

Element	Melting point [°C] [24]	D in Al at 400°C [m^2/s^{-1}] [25]	Atomic radius [Å]	Maximum solid solubility in Al in at.% [26]
Al	660.1	$3.25x10^{-15}$ (self-diffusion)	1.820	–
Fe	1536.0	$5.41x10^{-18}$	1.720	0.026
Mn	1244.0	$6.24x10^{-19}$	1.790	0.92
Cr	1857.0	$1.29x10^{-21}$	1.850	0.42
V	1902.0	$4.85x10^{-24}$	1.920	0.2
Ti	1667.0	$7.39x10^{-22}$	2.000	0.8
Zr	1852.0	$1.20x10^{-20}$	2.160	0.07
Mo	2620.0	$5.52x10^{-23}$	2.010	0.07

TEM studies confirm that the microstructure of all investigated melt spun ribbons is composed of aluminium solid solution matrix with the quasicrystalline particles identify as the icosahedral type based on 2, 3 and 5-fold selected area diffraction patterns (SADP). As an example, TEM bright field image of AlMnFeCr ribbon showing the quasicrysalline particles with the size of about 0.5 μm and 5-fold SADP obtained from a single particle are presented in Fig. 4. Composition of the quasicrystalline phase and the matrix determined by the EDX for all investigated alloys is given in Table 3. For all ribbons the quasicrystalline particles are enriched in Mn and Fe. The content of manganese varied from about 10 at.% in the case of Mo, Ti, Cr, V to about 12 at.% for AlMnFeZr and ternary AlMnFe alloy, while the iron content is in the range of 3.5-5 at.% for all alloys. The obtained values clearly revealed that zirconium is not present in the quasicrystals as was mentioned before, while the content of other adalitions was about 2 at.%. The matrix was enriched only in Mn (up to 2 at.%), except of AlMnFeZr ribbon, which additionally contained about 2 at.% of Zr.

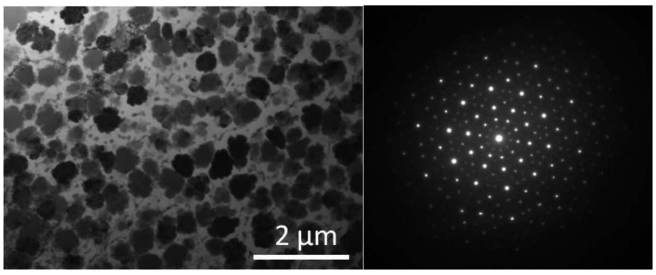

Fig. 4. Bright field TEM image of $Al_{91}Mn_6Fe_2Cr_1$ melt spun ribbon and SADP taken from one of the observed particles revealing 5-fold symmetry

TABLE 3
Mean chemical composition in at% of the icosahedral phase and matrix in melt spun ribbons together with the standard deviations

Alloy designation	Investigated area	Al	Mn	Fe	X
AlMnFe	Quasicrystal	82.8±1.4	12.5±1.0	4.7±0.4	–
	Matrix	97.5±1	2.30.7	–	–
AlMnFeMo	Quasicrystal	84.7±1.3	9.8±1.0	3.5±0.6	2.0±0.8
	Matrix	98.2±0.7	1.6±0.3	–	–
AlMnFeCr	Quasicrystal	82.6±1.9	10.4±1.5	5.0±0.6	2.0±0.5
	Matrix	96.0±1.1	2.4±0.8	1.3±0.4	–
AlMnFeTi	Quasicrystal	84.5±0.9	10.2±0.7	3.9±0.3	1.4±0.2
	Matrix	97.4±1.1	2.2±0.4	–	–
AlMnFeV	Quasicrystal	83.7±0.9	10.6±0.6	3.8±0.5	1.9±0.2
	Matrix	98.1±0.4	1.9±0.2	-	-
AlMnFeZr	Quasicrystal	82.5±1.6	12.0±1.4	5.3±1.0	-
	Matrix	96.5±1	1.5±0.4	–	2±1.0

In order to determine thermal stability of the quasicrystalline phase DSC analysis was performed. The as spun ribbons were heated up to 650°C with the rate of 40 K/min. For all the ribbons, one well noticeable exothermic peak is visible (Fig. 5). By comparing the curves obtained for the samples with different composition, shifts of this main exothermic peak is observed. This peak is connected with transformation of the metastable quasicrystals into stable crystalline phase during heating. Some of the curves have more complex run and contain additional small exothermic peaks revealing formation of some other phases during heating. Taking into account both main peak position and the presence of additional exothermic reactions occurring in the samples, it was concluded that the best thermal stability exhibits alloy with Mo addition. For this alloy the main exothermic peak shifts of about 100°C towards higher temperatures (in comparison with the ternary alloy) with almost no occurrence of additional reactions.

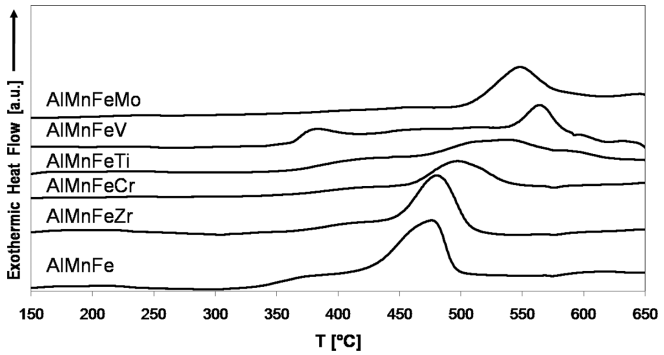

Fig. 5. DSC curves for all of the ribbons showing shift of the main exothermic peak position for different alloys composition

Vickers microhardness was measured on the ribbons cross sections for both typical areas observed in the sample (with small or large particles). Up to 20 indentations were performed for each sample. On the graphs (Fig. 6), average values obtained separately for both regions are marked (A and B similarly as in the Fig. 1-2) together with standard deviations. Additionally the average value calculated for both measurements is given for each sample. The region with fine particles always exhibits much higher microhardness than those obtained for the areas with larger particles. The highest microhardness for both areas was obtained for the sample with Zr addition and reaches mean value of over 270 μ HV_{100}. This result is due to the fact that zirconium remains in the matrix (probably in the form of precipitates) and causes additional strengthening of the alloy.

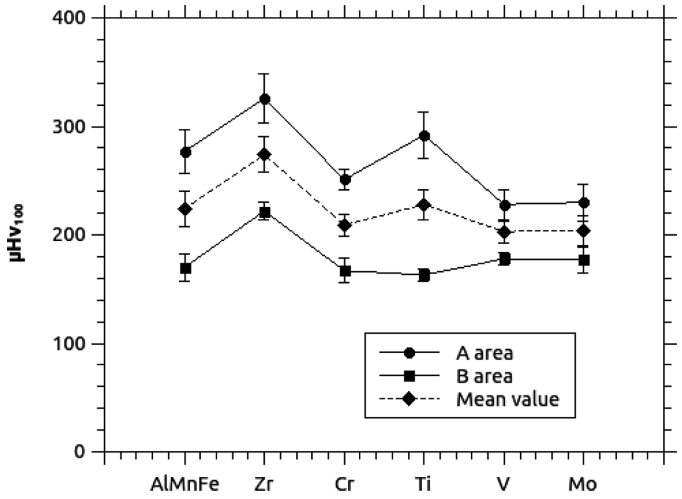

Fig. 6. Microhardness tests at room temperature for the as spun ribbons with addition of different transition metals. For each composition values for area A (fine spherical quasicrystalline particles) and area B (large particles) were measured

4. Conclusions

In this work influence of subsequent alloying elements on the microstructure and mechanical properties of the melt spun $Al_{91}Mn_7Fe_2$ alloy has been studied. The results revealed that the addition of fourth element (transition metal: Zr, Cr, Ti, V, and Mo) to the ternary alloy do not change the alloy microstructure and phase composition. All investigated ribbons contained quasicrystalline phase of icosahedral type in a form of spherical or dendritic particles with different sizes (from hundreds of nm to few micrometers) embedded in aluminium matrix. Size and shape of quasicrystalline particles depend strongly on cooling rates within the ribbon during solidification. Chemical analysis of both phases observed in the samples revealed that quasicrystalline phase always contains similar amounts of Al, Fe and Mn with small amount (up to 2%) of fourth element except of alloy with Zr addition. Chemical analysis of the latter showed that Zr is localized in the grains of aluminium matrix resulting in additional strengthening of the alloy. Therefore for this alloy the highest values of microhardness were obtained. DSC studies showed that the thermal stability of the alloys change with composition. Analysis of the main exothermic peak position as well as occurrence of other exothermic reaction in the sample showed that the best stability exhibits alloy with the Mo addition. It is not surprising since this element has one of the lowest diffusion coefficient in aluminium from the used additions and also the highest melting temperature.

Acknowledgements

The work was supported through project no. POKL. 04.01.00-00-004/10 co-financed by the European Union within the European Social Fund and project Polonium no.8415/2011.

REFERENCES

[1] M. Galano, F. Audebert, A. Garcia-Escorial, I.C. Stone, B. Cantor, J. Alloy. Compd. **495**, 372 (2010).
[2] M. Cavojsky, M. Baloga, J. Dvorak, E. Illekova, P. Svec, P. Krizik, D. Janickovic, F. Simancik, Mater. Sci. Eng. A **549** (2012).
[3] D. Vojtěch, A. Michalcová, F. Průša, K. Dám, P. Šedá, Mater. Charact. **66**, 83 (2012).
[4] A. Inoue, M. Watanabe, M.H. Kimura, F. Takahashi, A. Nagata, T. Masumoto, Mater Trans JIM **33**, 723 (1992).
[5] A. Inoue, H. Kimura, Materials Science and Engineering A **286**, 1 (2000).
[6] J.R. Davis, J.R. Davis, Aluminum and Aluminum Alloys, Technology & Engineering, 67 (1993).
[7] J.A. Lee, Automotive Alloys 2003, The 132nd TMS Annual Meeting & Exhibition San Diego Convention Center, San Diego, CA March 2-6, (2003).
[8] T. Tokuoka, T. Kaji, T. Nishioka, A. Ikegaya, Sei Technical Review **61**, 70 (2006).
[9] S.H. Choi, S.Y. Sung, H.J. Choi, Y.H. Sohn, B.S. Han, K.A. Lee, Procedia Engineering **10**, 159 (2011).
[10] M. Galano, F. Audebert, I.C. Stone, B. Cantor, Acta Materialia **57**, 5107 (2009).
[11] A. Michalcová, D. Vojtěch, G. Schumacher, P. Novak, M. Klementova, J. Serak, M. Mudrova, J. Valdaufova, Kovove Mater. **48**, 1 (2010).
[12] A. Inoue, H.M. Kimura, Nanostruct. Mater. **11**, 221 (1999).
[13] H.M. Kimura, K. Sasamori, A. Inoue, Mater. Sci. Eng. A **294-296**, 168 (2000).
[14] F. Audebert, F. Prima, M. Galano, M. Tomut, P.J. Warren, I.C. Stone, B. Cantor, Mater. Trans. **43**, 2017 (2002).

[15] M. Tomut, F. Prima, G. Huenen, G. Vaughan, A.R. Yavari, P. Svec, I.C. Stone, B. Cantor, Mater. Sci. Eng. A **375-377**, 1239 (2004).
[16] M. Yamasaki, Y. Nagaishi, Y. Kawamura, Scripta Mater. **56**, 785 (2007).
[17] M. Galano, F. Audebert, A. Garcia Escorial, I.C. Stone, B. Cantor, Acta Materialia **57**, 5120 (2009).
[18] F. Zupanic, T. Boncina, A. Krizman, W. Grogger, Ch. Gspan, B. Markoli, S. Spaic, J. Alloy Compd. **452**, 343 (2008).
[19] D. Vojtˇech, K. Saksl, J. Verner, B. Bartova, Mater. Sci. Eng. A **428**, 188 (2006).
[20] F. Schurack, J. Eckert, L. Schultz, Acta mater. **49**, 1351 (2001).
[21] A. Inoue, H. Kimura, K. Sasamori, T. Masumoto, Mater Trans JIM **37**, 1287 (1996).
[22] K. Stan, L. Lityńska-Dobrzyńska, J. Dutkiewicz, Ł. Rogal, A.M. Janus, Solid State Phenom. **186**, 255 (2012).
[23] K. Stan, L. Lityńska-Dobrzyńska, A. Góral, A. Wierzbicka-Miernik, Arch. Metall. Mater. **57**, 651 (2012).
[24] W.F. Gale, T.C. Totemeier, Smithells Metals Reference Book, Elsevier, Amsterdam, 2004.
[25] K.E. Knipling, D.C. Dunand, D.N. Seidman, Z. Metallkd. **96**, 246 (2006).
[26] E.J. Lavernia, J.D. Ayers, T.S. Srivatsan, Int. Mater. Rev. **37**, 1 (1992).

Received: 20 January 2013.